Submitted to Health Physics

RECEIVED
LAWRENCE
RADIATION LABORATORY

UCRL-20675
Preprint c.2

DOCUMENTS SECTION

MEASUREMENT OF HIGH-LET PARTICLES ON BIOSATELLITE III

E. V. Benton, S. B. Curtis, R. P. Henke, and C. A. Tobias
DONNER LABORATORY

May 1971

AEC Contract No. W-7405-eng-48

TWO-WEEK LOAN COPY

This is a Library Circulating Copy which may be borrowed for two weeks. For a personal retention copy, call Tech. Info. Division, Ext. 5545

UCRL-20675 c.2

LAWRENCE RADIATION LABORATORY
UNIVERSITY of CALIFORNIA BERKELEY

DISCLAIMER

This document was prepared as an account of work sponsored by the United States Government. While this document is believed to contain correct information, neither the United States Government nor any agency thereof, nor the Regents of the University of California, nor any of their employees, makes any warranty, express or implied, or assumes any legal responsibility for the accuracy, completeness, or usefulness of any information, apparatus, product, or process disclosed, or represents that its use would not infringe privately owned rights. Reference herein to any specific commercial product, process, or service by its trade name, trademark, manufacturer, or otherwise, does not necessarily constitute or imply its endorsement, recommendation, or favoring by the United States Government or any agency thereof, or the Regents of the University of California. The views and opinions of authors expressed herein do not necessarily state or reflect those of the United States Government or any agency thereof or the Regents of the University of California.

MEASUREMENT OF HIGH-LET PARTICLES ON BIOSATELLITE III*

E. V. BENTON,† S. B. CURTIS, R. P. HENKE,† and C. A. TOBIAS

Donner Laboratory, Lawrence Radiation Laboratory
University of California, Berkeley, California 94720

Abstract—High-LET particles encountered during the flight of Biosatellite III were measured by means of a detector packet consisting of tissue-equivalent plastic nuclear track detectors and nuclear photographic emulsions located in the proximity of the animal's brain. The plastic detectors were used to record $Z \geq 2$ particles, with track lengths, $L_0 > 10\ \mu$. Some charge resolution, even for the very short track segments $\approx 10\ \mu$, was found possible. A heavy recoil track density $\rho_R(Z > 2,\ L_0 > 10\ \mu) \approx 10^3\ cm^{-3}\text{-}day^{-1}$ was measured. This value is in good agreement with a predicted density calculated with the assumption that the tracks are caused by nuclear recoils produced through the inelastic scattering of the trapped protons. The measured results probably correspond only to the high energy tail of the total recoil track distribution.

---

* Work supported by NASA Ames Research Center, Moffett Field, California and U. S. Atomic Energy Commission.

† Permanent address: Physics Department, University of San Francisco, San Francisco, California 94117.

1. INTRODUCTION

The Biosatellite III flight, launched from Cape Kennedy on June 28, 1969, placed a 6-kilogram Macaca nemestrina primate in a nearly 200-nautical-mile circular equatorial orbit with inclination of 33.5°. The objective was to study the effects of the space environment on some of the basic biological processes.[1] Present in the space environment is a complex mixture of ionizing radiations. Of particular interest is the heavy-particle component, because of the possible high-LET effects on living organisms.

A special detector packet consisting of plastic nuclear track detectors and nuclear photographic emulsions was utilized to measure the high-LET component of particulate radiation. The packet was incorporated into the headrest of the animal-restraining couch so as to be located in the proximity of the animal's brain. A packet identical to the one flown served as a ground control. Because of their tissue equivalence, plastic detectors were used to measure the proton-induced inelastic recoil densities and charge distributions. In this paper the results are presented and compared with the calculated predictions.

2. DESCRIPTION OF THE EXPERIMENT

A detector packet of about 120 cm^2 area was used. It consisted of two types of plastic detectors--Lexan (polycarbonate) and Triafol TN (cellulose triacetate)--and two types of nuclear emulsions--Ilford G.5 and G.2. The sandwich arrangement of layers is shown in Table 1. The Lexan and Triafol plastics had a nominal thickness of 10 mils,

and the emulsions were nominally 100 microns thick.

The flight time was 8.5 days rather than the planned time of 30 days. The flight was terminated early because of the physiological deterioration experienced by the animal during the first 7 days.

After the flight, the Lexan detectors were first given a standard uv treatment[2] of 10-20-10 hours from sides 1-2-1, respectively, and etched for 4 hours in 70.4° C, 6.25 N NaOH with 0.5% Benax. From each surface a 10-μ-thick layer was removed, giving an average bulk etch rate, $V_G = 2.50$ μ per hour.

The Triafol, which was not given a uv treatment, was etched for 52.8 hours at 50.0° C in a solution composed of 6.25 N NaOH (75%) and a 12% NaClO solution (25%). A thickness of ≈ 62 μ was removed from each surface, giving $V_G = 1.17$ μ/hour.

Nuclear emulsions were developed by use of techniques described by Ilford.[3] The G.2 emulsions were developed in the standard way, whereas the G.5 emulsions were purposely severely underdeveloped in order to reduce the high background density of proton tracks.

Both sets of detectors were scanned by means of an optical microscope under 100× magnification. All measurements were made under 600× magnification.[4]

3. MEASUREMENTS

Track selection criteria

To facilitate the computation of the recoil track densities, ρ_R, and the charges, Z, of track-producing particles from the measurements in the plastic detectors, several simplifying conditions were imposed

as selection criteria:

1. The track-producing particle trajectories must be completely contained within the plastic prior to etching. Some bulk etching must take place before the track etching begins.

2. Tracks must be completely etched out. Tracks having sharp vertices (underetched) were not included.

3. The etched tracks must undercut the plastic surface; that is, there must be some portion of the track which can only be viewed through the plastic above it.

These three criteria are illustrated in Figs. 1 and 2. Figure 1 shows the various possible particle trajectories. Trajectory (a) is the only acceptable one. Trajectory (b) does not meet criterior 1. Although (c) appears to meet the requirements, in reality it fails criterion 3. The etched track will be similar to track (d) in Fig. 2. Trajectory (d) fails both criteria 1 and 3. Obviously trajectory (e) can produce no track at all with the amount of etch shown. It is possible for either (a) or (b) to not meet criterion 2 if the track etch rate, V_T, is sufficiently small. Also shown in the figure are L_0, the particle trajectory length, and B, the thickness of the surface layer removed through bulk etch.

In Fig. 2 are shown the various possible types of etched tracks. The dip angle, δ, and cone angle, θ, are shown in (a), which is the only acceptable track. Track (b) fails criterion 2. Track (c) fails criterion 3 because $\delta > (\pi/2 - \theta)$. Track (d) results from a trajectory of type (c) or (d) in Fig. 1 and fails criterion 3. Track (e) fails both criteria 2 and 3.

It can be seen that criteria 2 and 3 can be applied by merely inspecting the track. If the thickness of material removed through bulk etch, B, is greater than the longest possible trajectory, criterion 1 is met by all tracks. Otherwise the particle track must be completely measured to determine if criterion 1 is met.

Etch rate calibration

The relationship between the track etch rate, V_T, and the particles' LET[5] was established using Hilac accelerated particles (see Figs. 3 and 4). The Lexan calibration was taken to be the previously measured relationship

$$V_T = 196(\mathrm{LET})^{2.38} \quad \mu/\mathrm{hour}. \tag{1}$$

In Triafol the calibration was obtained by successively etching ^{16}O and ^{20}Ne tracks. The experimental points are shown in Fig. 4 and can be fitted by the expression

$$V_T = 30.4(\mathrm{LET})^{1.54} \quad \mu/\mathrm{hour}. \tag{2}$$

LET is given in MeV/μ.

Scanning and measurement

In Lexan 21.7 cm^2 was scanned by scanner A and 8.39 cm^2 of this area was also scanned by scanner B. This was done at 100× magnification. Scanner A scanned with horizontal continuous motion, whereas B scanned with vertical stepwise motion. On the basis of stipulating only criterion 3, a total of 88 tracks were found. In Triafol 7.96 cm^2 was scanned at 100× with vertical stepwise motion by scanner B. Both

selection criteria 2 and 3 were employed and 20 tracks were found. Criterion 1 was met because of the large value of B.

The values of the cone angles, θ, the track etch rate, V_T, the depth of the top of the track, and the track length, L, were measured and computed. In Lexan the value of V_T includes the correction for uv attenuation with depth. For those tracks meeting criteria 1 and 2 it is possible to state that $L = L_0$.

Of the 88 tracks found in Lexan, 4 failed to meet criterion 1 alone, 10 failed to meet criterion 2 alone, and 9 failed to meet both criteria 1 and 2. Thus the number of tracks available for track density and charge measurement was 65.

Determination of recoil atomic number, Z

All tracks satisfying the selection criteria are plotted in Figs. 5 and 6. On these V_T vs L_0 plots, curves corresponding to the various possible recoil types are also included. The identity of each recoil can be determined by comparison of the points with the curves. (Only one isotope for each element is plotted since curves of the other possible isotopes lie very close together.) Element Be was not included because the probability of its production is extremely small.

The curves of V_T vs L_0 shown in Figs. 5 and 6 were based on the etch-rate calibrations given in equations (1) and (2) and the range-LET relationships for Lexan and Triafol. In these plots it is assumed that the average etch rate measured is the etch rate at the average residual range, $\bar{R}$. Since criteria 1 and 2 have been satisfied, $L_0 = L$, and thus $\bar{R} = 1/2\ L_0 = 1/2\ L$.

The accuracy of the determination of the recoil atomic number varies considerably over the region of Figs. 5 and 6. Those points along the top edge of Fig. 5 have been measured, and lie somewhere above the plotted values, but because of the large experimental uncertainty they may be as light as boron. For events which result in very short tracks with large values of V_T, the experimental uncertainty in charge determination is large. Thus, there is no real discrimination within the B-C-N group. However, certainly those events in the B-C-N group can be separated from the Li group. A large group of Li points is evident in Fig. 5. In Fig. 6 there are also three points ascribed to He.

Scanning efficiency

To convert the measured track fluences in tracks/cm^2 into realistic, objective fluence values, the scanning efficiency must be determined. The efficiencies of scanners A and B were determined from the portion of the Lexan sheet scanned by both scanners. These efficiencies are given in Table 2 as a function of the track length.

Measured recoil densities

The recoil densities, ρ_R, are given by

$$\rho_R = \frac{2\sigma}{L_0(1 - \sin 2\theta)}, \quad \text{for} \quad L_0 < \frac{B}{\cos\theta}, \tag{3}$$

and

$$\rho_R = \frac{\sigma}{(B - L_0 \sin\theta)[\cos\theta - (1/2)\sin\theta - (1/2)B/L_0]},$$

$$\text{for} \quad L_0 > \frac{B}{\cos\theta}, \tag{4}$$

where σ = the corrected recoil fluence,
B = the thickness removed through the bulk etch,
L_0 = the trajectory length, and
θ = the track cone angle.

Formulae (3) and (4) take into account the effective registration volume and the fraction of tracks that are not included by virtue of the selection criteria. The assumptions behind these formulae are: (i) that both the recoil trajectory direction and the detector sensitivity are isotropic, and (ii) that the etch time is sufficient to completely etch out a track of length L_0 that etches for the full etch time.

For Lexan, formula (4) was applied to groups of tracks with similar values of L_0 and θ. The few tracks with $L_0 < 10\ \mu$ were excluded to make the comparison with the calculated results meaningful (see section 4). Also, the scanning efficiencies are not known for $L_0 < 10\ \mu$. For Triafol formula (3) was applied to each track individually.

Table 3 gives the measured values of ρ_R for each ion or group of ions. Here N is the number of tracks and the uncertainties given are those arising from counting statistics alone.

Integral LET spectrum

The integral LET spectrum

$$\frac{d^2N(LET > LET_0,\ L_0 > 10\ \mu)}{dA\ d\Omega},$$

the number of particles $cm^{-2}\ sr^{-1}$ with $LET > LET_0$ and $L_0 > 10\ \mu$, is shown in Fig. 7. The abscissa variable is LET_0 in MeV/μ transferred to electrons with recoil energies < 350 eV. The integral LET spectrum is obtained from

$$\frac{d^2N(LET > LET_0,\ L_0 > 10\ \mu)}{dA\,d\Omega} = \frac{1}{4\pi} \sum_{LET_i > LET_0} L_{oi}\rho_i \qquad (5)$$

by summing over individual tracks for Triafol and groups of tracks having similar values of L_0 and V_T for Lexan. L_{oi} is the length (distance from the interaction point to the stopping point of the recoil) of the track or the average length for the group of tracks. The quantity ρ_i is the density (in particles/cm^3) represented by the track or group of tracks, and LET_i is the value of LET corresponding to the average value of V_T. The differential of area, dA, is the element of projected area, the area normal to the beam direction. The differential $d\Omega$ is the element of solid angle. Equation (5) assumes an isotropic distribution of recoil trajectories.

For $LET < LET_c$ the etched tracks have $\theta > \pi/4$. Since $\delta > \theta$ is necessary for registration, these tracks will not be undercut and will be rejected by selection criterion 3.

Observation in nuclear emulsions and plastics

Examination of the nuclear emulsions revealed a high background of tracks due to singly charged and multicharged particles. Locations of the tracks due to the primary heavy particles were noted. An example of the heaviest track observed in emulsion appears in the center of Fig. 8. Attempts were made to trace these into the adjacent layers of plastic detector. No corresponding tracks were found in the plastic.

After the sensitizing uv treatment, the sensitivity of Lexan is such that the following particle types can be detected: $Z = 6$ with $E \lesssim 6$ MeV/amu,

$Z = 26$ with $E \lesssim 250$ MeV/amu, $Z \geq 37$ with $E \lesssim 2.5$ GeV/amu. The Triafol detector is somewhat more sensitive than the sensitized Lexan. Tracks due to primary high-Z particles were not observed in either detector. These observations are consistent with the high geomagnetic cutoff for this particular orbit and the relatively small value of the area-time factor achieved.

Nuclear emulsions were examined for the recoil tracks observed in plastics. Although undoubtedly present, it was not possible to distinguish them from the very high density of background grains present, or from the numerous tracks of singly charged particles (see Fig. 8).

Observations in the nose cone aluminized Mylar

A layer of aluminized Mylar located directly behind the heat shield of the spacecraft was also examined for tracks. This material formed an integral part of the spacecraft. Being nearly 1 m^2 in area, it was large enough to record the passage of rare, primary, very-high-z particles. Unfortunately this material was found unsuitable for particle detection.

4. CALCULATIONS

Estimation of the expected recoil density

In principle, it is possible to calculate the number of nuclear recoils per unit volume, with length greater than a certain distance. The physical quantities necessary for such a calculation are

(i) the fluence (no./cm^2) of incident particles traversing the plastic;

(ii) the cross sections for production of the nuclear recoils; and

(iii) an estimate of the fractional number of each type of recoil that produces tracks long enough to be detected.

The equation for the recoil density (no./cm^3) with track lengths greater than some distance L_0 is

$$\rho_R(>L_0) = \frac{N_0 \rho \Delta T}{M} \left\{ n_c \int \left[\Sigma_i \, \sigma_{ic} \, F_{ic} \, (>L_0) \right] \frac{d^3N}{dAdEdt} \, dE \right. \\ \left. + \; n_{ox} \int \left[\Sigma_i \, \sigma_{iox} \; F_{iox} \, (>L_0) \right] \frac{d^3N}{dAdEdt} \, dE \right\}. \tag{6}$$

Here

N_0 = Avogadro's number (molecules/mole),

ρ = density of the plastic (g/cm^3),

ΔT = spaceflight duration (sec),

M = molecular weight of the plastic (g/mole),

n_c = number of carbon atoms per molecule,

n_{ox} = number of oxygen atoms per molecule,

σ_{ic} = cross section for production of the ith type of recoil on carbon (cm^2),

σ_{iox} = cross section of production of the ith type of recoil on oxygen (cm^2),

$F_{ic}(>L_0)$ = fraction of recoils of the ith type which go at least a distance L_0 from carbon interaction,

$F_{iox}(>L_0)$ = fraction of recoils of the ith type which go at least a distance L_0 from an oxygen interaction, and

$d^3N/dAdEdt$ = differential energy spectrum of the particles producing recoils (no./cm^2-MeV-sec).

The only two possibilities for the source of particles producing the recoils are protons from the trapped radiation belts and the galactic protons. No solar-particle events occurred during the flight. The following calculation is for trapped protons only.

The trapped-proton environment was estimated as follows. The average daily spectrum was calculated by using the Boeing-developed integration program, which integrates the spectrum over the B and L space traversed by the vehicle trajectory. In one day, all inhomogeneities are approximately averaged out and the daily spectrum can then be multiplied by the number of days the flight lasted to obtain the average time-integrated energy spectrum. This spectrum must then be degraded by the shielding of the spacecraft itself. Since a shielding distribution was not known for the position of the plastic-emulsion packet, it was decided to calculate the recoil density assuming three different thicknesses of spherical spacecraft shielding: 2, 5, and 10 g/cm^2 of aluminum. The true density undoubtedly lies somewhere within this rage. The degraded spectra were calculated with the Boeing shielding code.[6]

The cross sections for recoil production were obtained from the Monte Carlo codes developed by Oak Ridge National Laboratory.[7] Three energies of incident protons were used: 50, 100, and 200 MeV. The results give the production cross sections for recoils of different types from nuclear interactions of protons of the above energies on carbon and oxygen. Also, the average energy of each type of recoil was obtained at each energy. The energy spectra of the recoils, however, were not obtained. It was decided to use the shape of the α-particle spectrum and renormalize it so that the average recoil energy was

obtained for the first moment of the distribution. These renormalized spectra were then integrated to give the fractional number of recoils with energies greater than a given energy per nucleon, for the various recoil types. From a range energy code developed for these plastics,[4] the F_{ic} and F_{iox} ($> 10\ \mu$) were determined by reading the values of the integral spectra for that energy per nucleon corresponding to a range of $10\ \mu$.

The values of cross sections F_{ic} and F_{iox} are given for the various recoil types, proton energies, and plastic constituents in Table 4. The average daily spectra at the three energies, shielding thicknesses, and the integrands [in equation (6)] for each shielding thickness, energy, and plastic constituent are also shown in Table 4.

The calculation was made for Lexan. The values used for the quantities in equation (6) were:

$\rho = 1.17\ g/cm^3$,

$M = 254$ g/mole (the molecular formula $C_{16}H_{14}O_3$ was used),

$T = 8.25$ days,

$n_c = 16$,

and

$n_{ox} = 3$.

The integrands in Table 5 were used to determine a rough dependence on energy. Since there were only three energy points, the dependence of the integrands could be only crudely estimated, and the resulting integral can be considered only a rough approximation. The results are given in Table 6 for the three shielding thicknesses. Because

of the crudeness of the calculation, only one significant figure is given.

5. CONCLUSION

Comparison of measured and calculated results

By use of equation (6), Lexan parameters, and the parameters $\rho = 1.24$, $M = 72$, $n_c = 3$, and $n_{ox} = 2$ for Triafol, it is found that the calculated values of recoil density given in Table 6 also hold for Triafol. Because of the large uncertainties involved it can be said that the calculated results in Table 6 agree with the measured Triafol results, but are slightly in disagreement with the measured Lexan results.

The predicted and measured recoil charge distributions are in excellent agreement within experimental error. They are given in Table 7.

The LET spectrum given in Fig. 7 is only an approximation of the true spectrum. This is because each LET value given is not the value at a single point on the recoil track but is the effective value of LET, the value necessary to produce the average preferential etch rate, V_T, which is the measurable quantity. Thus, although the maximum value of LET achieved by a nitrogen ion at its Bragg peak is 1.1 MeV/μ, no tracks are shown with effective LET values this high because all track segments were at least 10 μ long.

To ensure the health and safety of the astronauts it is important to possess as complete a picture of the radiation environment as possible. Although many previous measurements have been performed, this work represents the first measurement of the high-LET nuclear recoil component induced through inelastic proton scattering in a solid tissue-equivalent material. These measurements are possible only because

of the unique properties of plastic nuclear track detectors: (i) the ability to record only heavily ionizing particles while being unaffected by large backgrounds of more lightly ionizing radiations, and (ii) having a response with a strong dependence on ionization rate, thus permitting charge identification of very short track segments.

It should be noted that the sensitivity of plastic nuclear track detectors used in these measurements is such that they are heavily biased against particles as light as ^{4}He. However, the cross section for ^{4}He production is relatively high, and it is expected that the recoil track density for ^{4}He, $\rho(^4\text{He})$, is at least comparable to if not higher than the measured $\rho(\text{Li}+\text{B}+\text{C}+\text{N})$. Also, due to the nature of the detectors, the measured $\rho(L_0 > 10\ \mu)$ represents only the high-energy tail of the total recoil track density. It is expected that $\rho(L_0 > 1.0\ \mu) > \rho(L_0 > 10\ \mu)$. This is illustrated in Table 4, where for many types of recoils F_{ic}, $F_{io} << 1$. In fact, those recoil types with the smallest values of F_{ic} and F_{io} were selectively eliminated from Table 4 because they did not contribute significantly to $\rho_R(L_0 > 10\ \mu)$. Consequently the measured recoil density, $\rho_R(Z > 2,\ L_0 > 10\ \mu) \approx 10^3$ recoils cm^3 day^{-1}, may be only a small fraction of the total. It should also be pointed out that the integral LET recoil spectrum, shown in Fig. 7, is similar to the integral spectra of primary high-Z particles as obtained on the lunar Apollo missions.[8] Further measurements of this type utilizing presently available improved-sensitivity nuclear track detectors are needed to properly assess the biological implications of nuclear recoils.

Acknowledgments—The authors acknowledge their appreciation to A. L. Frank for performing some of the measurements and to Rollin Armer for help in designing the flight package. We also are grateful for the help of Dr. R. C. Alsmiller of the Neutron Physics Division of Oak Ridge National Laboratory in providing us with the cross section and energy spectrum calculations at 50, 100, and 200 MeV. We also thank Dr. R. Doherty, Space Sciences Group, The Boeing Company, for providing us with the time-integrated daily proton spectra for the Biosatellite III orbit, and M. C. Wilkinson, also of the Space Sciences Group, for the degraded proton spectra behind 2, 5, and 10 g/cm^2 shielding.

REFERENCES

1. W. R. ADEY, A. T. K. COCKETT, P. B. MACK, J. P. MEEHAM, and N. PACE, Science 166, 492 (1969).
2. R. P. HENKE, E. V. BENTON and H. H. HECKMAN, Radiation Effects 3(1), 43 (1970).
3. Technical Information Sheet U501, Ilford Limited, Ilford, Essex, England.
4. E. V. BENTON, A study of charged particle tracks in cellulose nitrate, USNRDL-TR-68-14 (1968).
5. We make the assumption that the track-etch rate, V_T, depends on Z and β through the quantity LET. The quantity LET as used in this paper is LET_{350}, the energy per path length of incident particle lost to electrons in energy-transfer collisions of less than 350 eV. Another name for this quantity is REL, the restricted energy loss rate. In the previous work, including reference (1), LET_{1000} was used. Recently we found LET_{350} to be a more realistic value.
6. R. DOHERTY and M. WILKINSON, private communication.
7. R. C. ALSMILLER, private communication.
8. E. V. BENTON and R. P. HENKE, High Z particle Apollo astronaut dosimetry with plastics. Presented at the National Symposium on Natural and Manmade Radiation in Space, Las Vegas, March 1971.

Table 1. Arrangement of detectors in the stack

Layer No.	Detector	Layer No.	Detector
1	Triafol	12	G.2
2	Triafol	13	Lexan
3	Triafol	14	G.5
4	Triafol	15	Lexan
5	Lexan	16	G.2
6	G.5	17	Lexan
7	Lexan	18	G.5
8	G.2	19	Lexan
9	Lexan	20	G.2
10	G.5	21	Lexan
11	Lexan	22	Lexan

Table 2. Scanning efficiencies

L_0	Scanner A	Scanner B
10.0-12.3 μ	0.348	0.445
12.3-20.3 μ	0.364	0.571
20.3-34.0 μ	0.320	1.000

Table 3. Recoil densities (tracks/cm^3)

	Lexan		Triafol	
Ion(s)	N	ρ_R (L_0 > 10 μ)	N	ρ_R (L_0 > 9 μ)
He			3	$12 \pm 9 \times 10^3$
Li	31	$9.2 \pm 7 \times 10^3$	10	$3.6 \pm 1.4 \times 10^3$
B + C + N	17	$2.4 \pm 0.5 \times 10^3$	7	$2.6 \pm 1.3 \times 10^3$
Li + B + C + N	48	$11.6 \pm 1.8 \times 10^3$	17	$6.2 \pm 1.9 \times 10^3$

Table 4. Tabulation of cross sections for various recoil types.

	50 MeV						100 MeV						200 MeV					
	Carbon			Oxygen			Carbon			Oxygen			Carbon			Oxygen		
Ion	σ_{ic} mb*	F_{ic} (>10μ)	$\sigma_{ic} F_{ic}$ (>10μ)	σ_{iox} (mb)	F_{iox} (>10μ)	$\sigma_{ic} F_{iox}$ (>10μ)	σ_{ic}	F_{ic}	$\sigma_{ic} F_{ic}$	σ_{iox}	F_{iox}	$\sigma_{iox} F_{iox}$	σ_{ic}	F_{ic}	$\sigma_{iox} F_{iox}$	σ_{ic}	F_{ic}	$\sigma_{ic} F_{ic}$
^{6}Li	18.89	0.275	5.195	1.02	0.2	0.204	11.61	0.26	3.019	3.24	0.5	1.62	9.29	0.3	2.787	3.07	0.5	1.535
^{10}B	52.50	0.032	1.68	5.11	0.08	0.409	34.53	0.018	0.622	5.97	0.145	0.866	28.80	0.004	0.115	8.01	0.215	1.722
^{11}B	22.30						22.61						30.82					
^{10}C	6.50						4.03						2.94					
^{11}C	74.02	10^{-4}	0.007	1.02	0.085	0.087	49.56	10^{-4}	0.005	3.58	0.155	0.555	47.08	10^{-4}	0.005	1.88	0.13	0.244
^{12}C	31.75	10^{-4}	0.003	76.04	0.0155	1.179	17.19	10^{-4}	0.002	59.50	0.0255	1.517	8.21	10^{-3}	0.008	44.33	0.051	2.261
^{13}C				21.82	0.028	0.611				12.28	0.0077	0.095				6.65	0.02	0.133
^{14}N				121.73	5×10^{-4}	0.061				70.24	10^{-4}	0.007				54.56	0.00145	0.079
SUM			6.885			2.551			3.648			4.66			2.915			5.974

* $1 mb = 10^{-27} cm^2$

Table 5. The average daily proton spectra at three energies and shielding thicknesses.

	Proton energy: 50 MeV			Proton energy: 100 MeV			Proton energy: 200 MeV		
Shielding Thickness g/cm, Al	Diff. Energy Spectrum	Integrands [in equation (6)]		Diff. Energy Spectrum	Integrands [in equation (6)]		Diff. Energy Spectrum	Integrands [in equation (6)]	
	no./cm^2-MeV-day	Carbon	Oxygen	no./cm^2-MeV-day	Carbon	Oxygen	no./cm^2-MeV-day	Carbon	Oxygen
		no. recoils / day-MeV-carbon nucleus	no. recoils / day-MeV-oxygen nucleus		no. recoils / day-MeV-carbon nucleus	no. recoils / day-MeV-oxygen nucleus		no. recoils / day-MeV-carbon nucleus	no. recols / day-MeV-oxygen
2	1.0493×10^{4}	7.2244×10^{-23}	2.6768×10^{-23}	5.9331×10^{3}	2.164×10^{-23}	2.765×10^{-23}	1.8069×10^{3}	5.267×10^{-24}	1.079×10^{-23}
5	5.8606×10^{3}	4.035×10^{-23}	1.495×10^{-23}	4.1976×10^{3}	1.531×10^{-23}	1.956×10^{-23}	1.512×10^{3}	4.407×10^{-24}	9.033×10^{-24}
10	2.9281×10^{3}	2.016×10^{-23}	7.470×10^{-24}	2.6044×10^{3}	9.5×10^{-23}	1.214×10^{-24}	1.1515×10^{3}	3.357×10^{-24}	6.879×10^{-24}

Table 6. Calculated $\rho_R (L_0 > 10\ \mu)$.

Shielding Thickness g/cm^2 Al	Carbon Integrals $\frac{\text{Number of coils}}{\text{day-carbon nucleus}}$	Oxygen Integrals $\frac{\text{Number of coils}}{\text{day-oxygen nucleus}}$	Recoil density $\rho(L>10_3)$ no./cm_3
2	6×10^{-21}	5×10^{-21}	3×10^3
5	4×10^{-21}	3.7×10^{-21}	2×10^3
10	2.6×10^{-21}	2.5×10^{-21}	1×10^3

Table 7

Values of $\frac{\rho_R (L_0 > 10\ \mu) \text{ for } (B+C+N)}{\rho_R (L > 10\ \mu) \text{ for } (Li+B+C+N)}$

	Lexan	TTN
Predicted	0.265	0.393
Measured	0.207 ± 0.068	0.419 ± 0.300

FIGURE CAPTIONS

Fig. 1. Different possible types of recoil-particle trajectories.

Fig. 2. Different possible types of etched particle tracks.

Fig. 3. Photomicrographs of 10-MeV/nucleon heavy-ion tracks in Lexan. The detectors were first sensitized with a uv treatment and then etched for 2.0 hr at 70.4° C in 6.25 N NaOH with 0.5% Benax.

Fig. 4. Track etch rate calibration in Triafol TN.

Fig. 5. Recoil identification in Lexan.

Fig. 6. Recoil identification in Triafol TN.

Fig. 7. Integral LET spectrum for tracks of $L_0 \geq 10\ \mu$.

Fig. 8. Photomicrograph of a section of G.5 emulsion. Track at center, probably of a fast iron particle, is of the heaviest type found in emulsion. No corresponding tracks were found in plastics. Tracks of recoils could not be distinguished from the very high density of background grains and other tracks present.

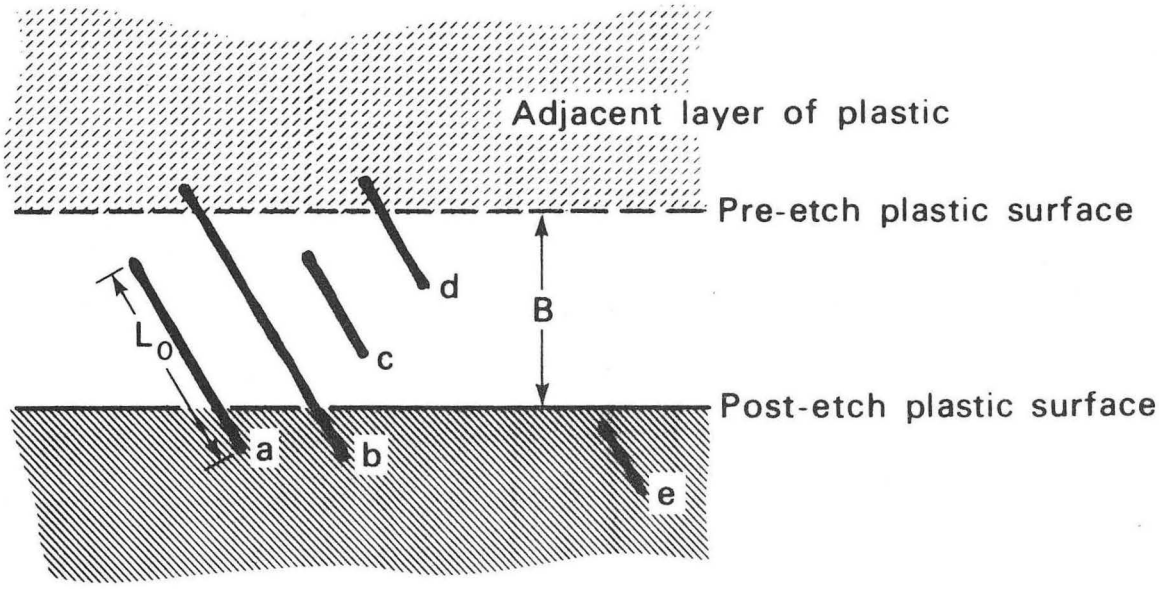

DBL 7011 6019

Fig. 1

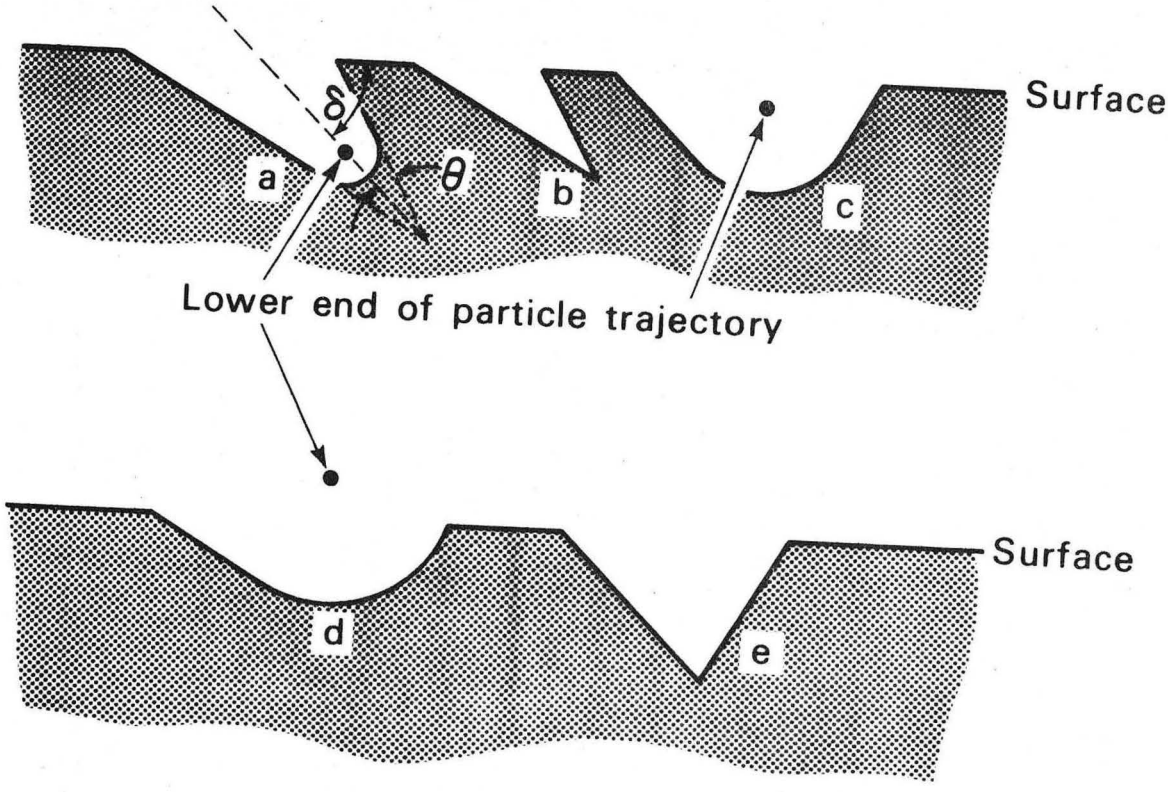

DBL 7011 6020

Fig. 2

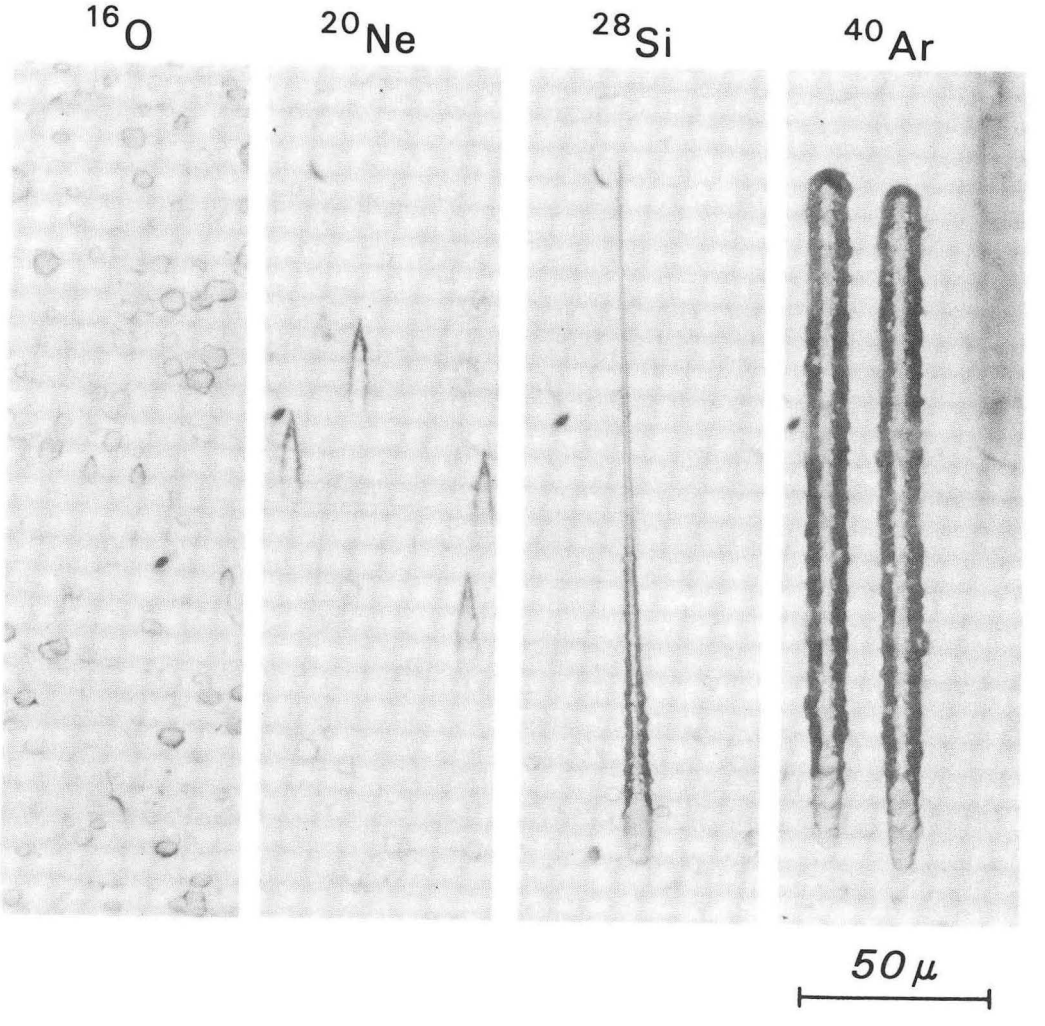

XBB 7010-4953

Fig. 3

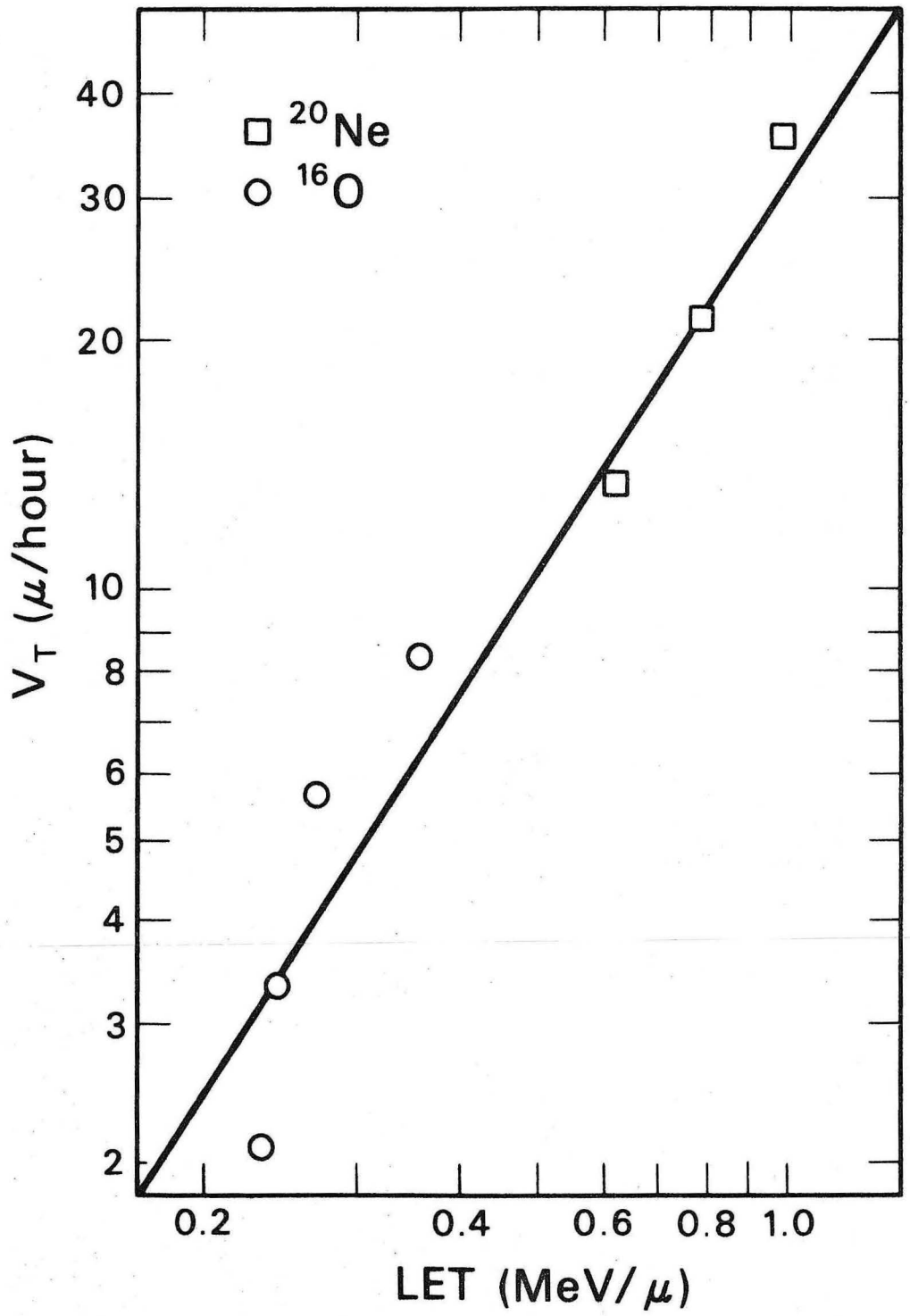

DBL 7011 6021

Fig. 4

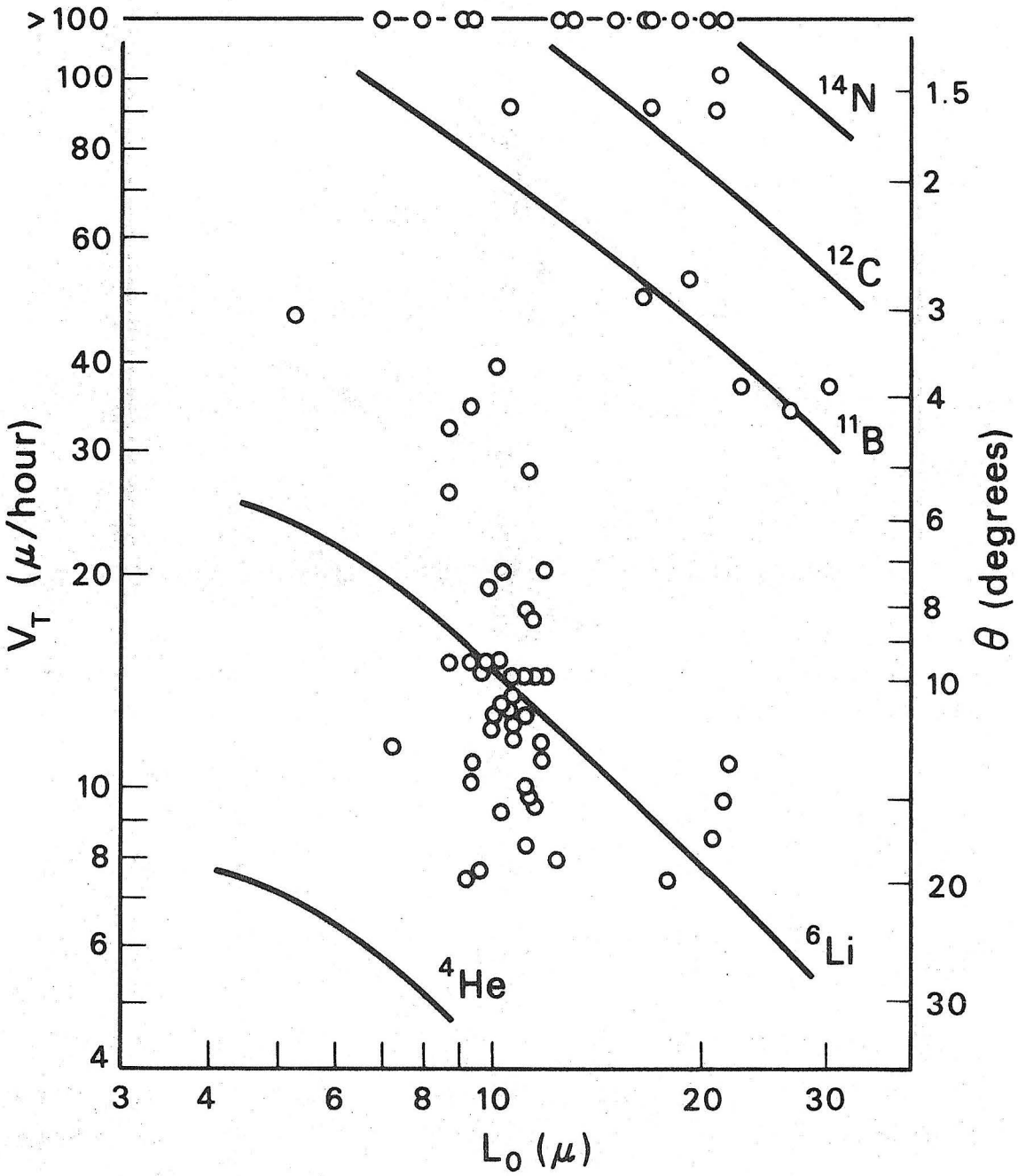

DBL 7011 6022

Fig. 5

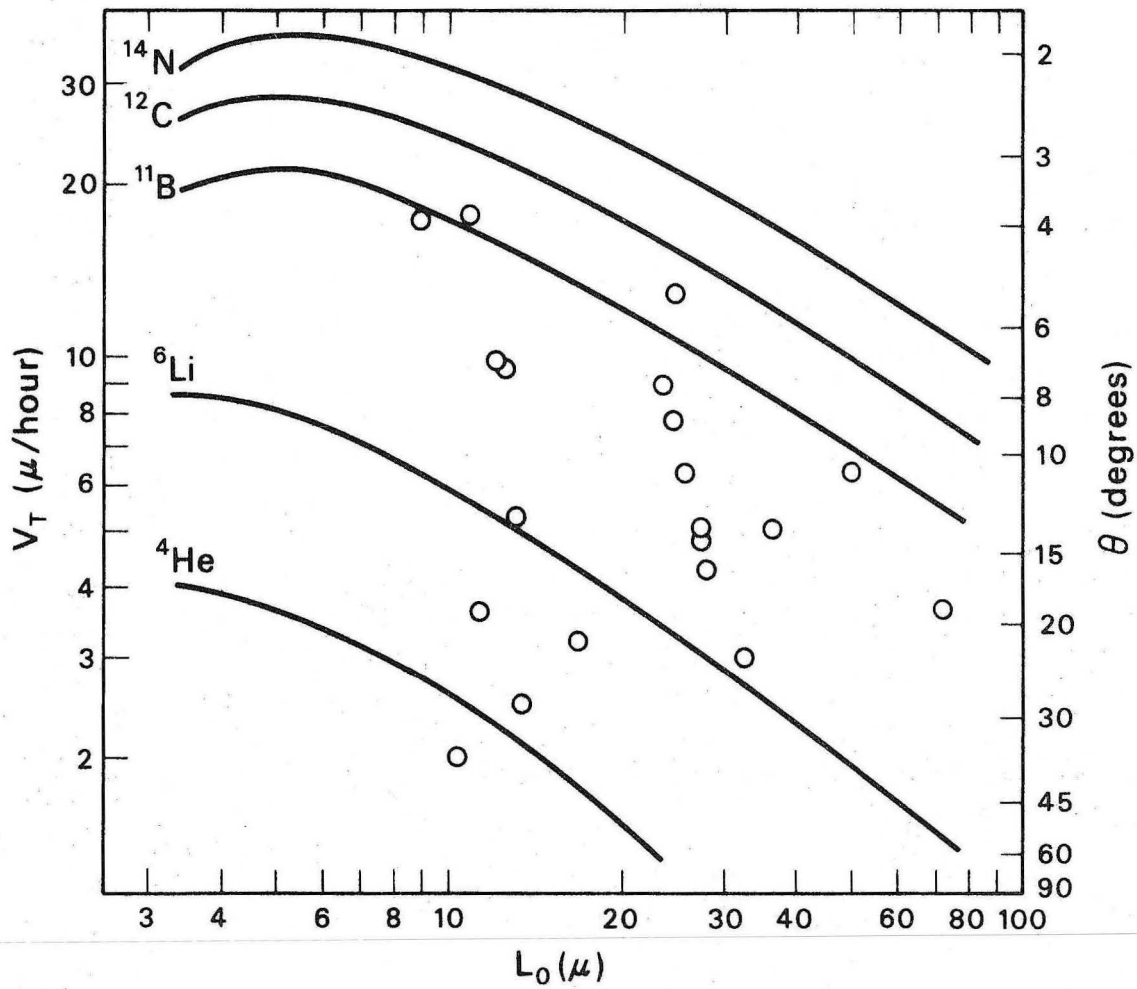

DBL 7011 6023

Fig. 6

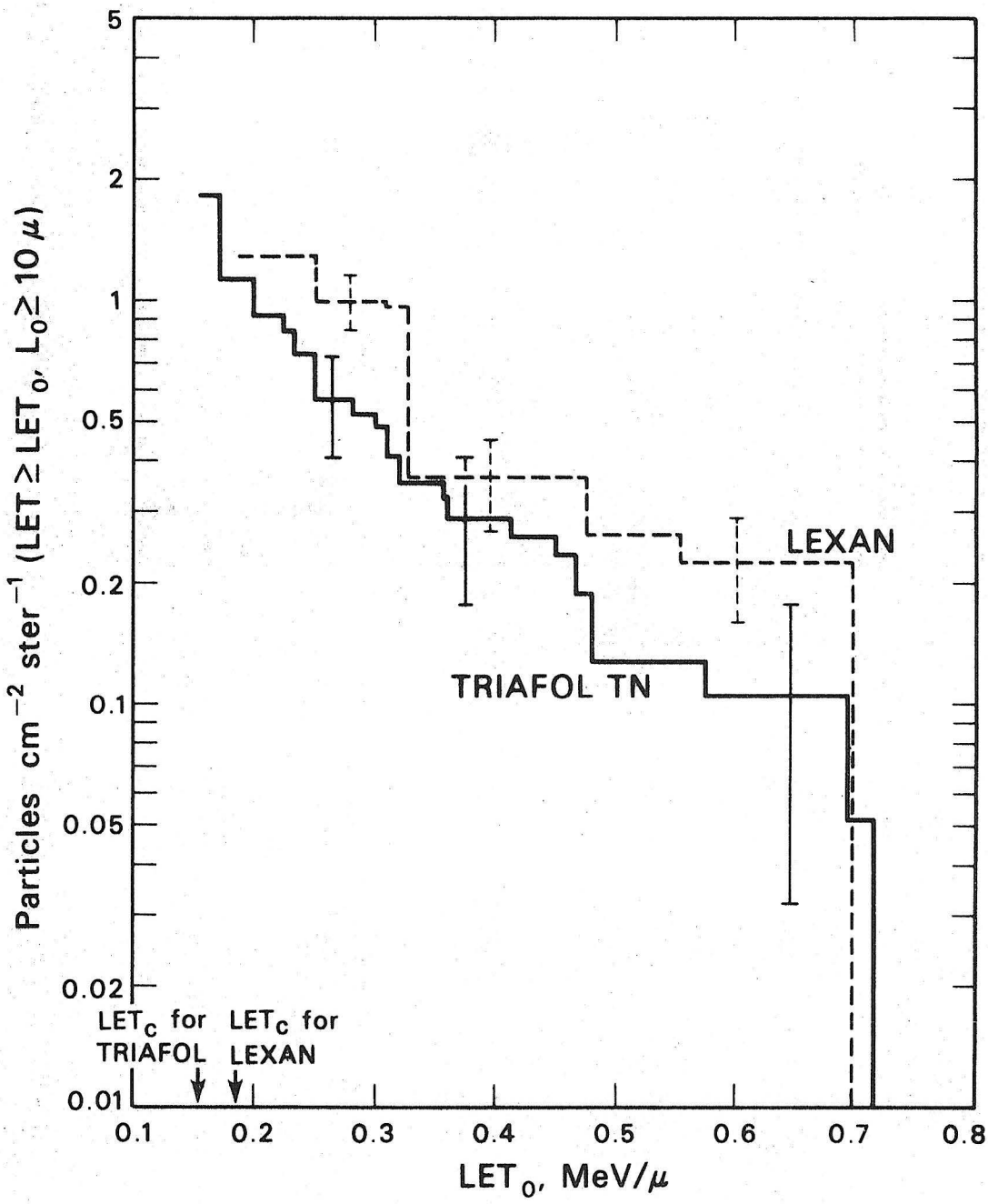

DBL 712 5666

Fig. 7

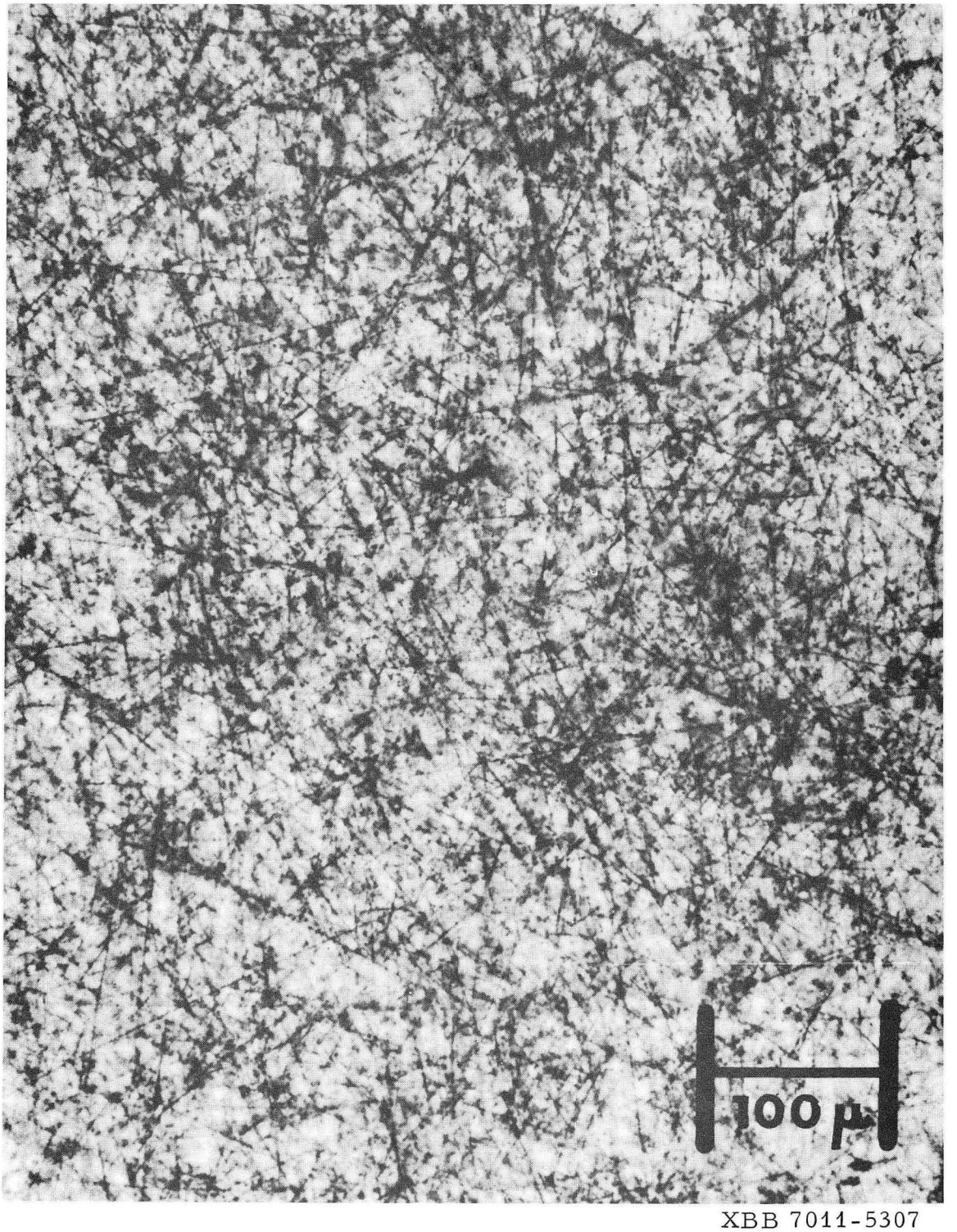

XBB 7011-5307

Fig. 8

LEGAL NOTICE

This report was prepared as an account of work sponsored by the United States Government. Neither the United States nor the United States Atomic Energy Commission, nor any of their employees, nor any of their contractors, subcontractors, or their employees, makes any warranty, express or implied, or assumes any legal liability or responsibility for the accuracy, completeness or usefulness of any information, apparatus, product or process disclosed, or represents that its use would not infringe privately owned rights.

TECHNICAL INFORMATION DIVISION
LAWRENCE RADIATION LABORATORY
UNIVERSITY OF CALIFORNIA
BERKELEY, CALIFORNIA 94720